A facial reconstruction method based on new mesh deformation techniques

Maya de Buhan, Chiara Nardoni

A facial reconstruction method based on new mesh deformation techniques.

Maya de Buhan[1*]

[1] *CNRS, UMR 8145, MAP5, Université Paris Descartes, Sorbonne Paris Cité, France*

Chiara Nardoni[2‡]

[2] *Sorbonne Universités, UPMC Univ Paris 06, Institut des Sciences du Calcul et des Données, F-75005, Paris, France*

Abstract

This article presents a new numerical method for facial reconstruction. The problem is the following: given a dry skull, reconstruct a virtual face that would help in the identification of the subject. The approach combines classical features as the use of a skulls/faces database and more original aspects: (i) an original shape matching method is used to link the unknown skull to the database templates; (ii) the final face is seen as an elastic 3d mask that is deformed and adapted onto the unknown skull. In this method the skull is considered as a whole surface and not restricted to some anatomical landmarks, allowing a dense description of the skull/face relationship. Also, the approach is fully automated. Various results are presented to show its efficiency.

Keywords: forensic science, facial reconstruction, shape matching, elasticity, soft tissue deformation, finite elements

*e-mail: maya.de-buhan@parisdescartes.fr

†e-mail: chiara.nardoni@upmc.fr

‡This work received a financial support by Idex Sorbonne Universités under the French funds "Investissement d'Avenir", reference ANR-11-IDEX-0004-02

Introduction

Facial reconstruction aims at recovering the facial appearance of an individual from the sole datum of the underlying skull. The facial reconstruction problem arises in various application fields like forensics, anthropology, archeology or history. In forensic science, facial reconstruction comes in the process of identification of deceased people. When all the usual methods of identification have failed and the skeletal remains are the sole data available for leading to a positive identification, facial reconstruction might be considered as an enhancing tool for 'recognition', producing a short list of candidates from which the individual may be identified by other endorsed methods of identification, see Wilkinson [1]. In archeological investigations, facial reconstruction is employed with the purpose of identifying skeletal remains of famous people from the past.

The creation of the face from the skull is a procedure of *approximation*: from the observation of the cranium, one will not be able to recover a large amount of face features (eyes, hair, lips, ears). Moreover the facial likeness of a given individual changes considerably depending on factors like nutrition or aging. This flexibility may not be fully reflected on the subjacent skull. Any facial reconstruction tool is expected to account for the uncertainty related to the *ill-posedness* of the problem, no matter what method is employed (artistic, parametric, statistic, mechanical, etc.). From a mathematical point of view, this issue leads to at least two important difficulties: on the one hand, it raises the question of how to correctly characterize the solution, which might be a continuum spectrum of all the faces that are 'consistent' with a given skull rather than a single exemplar; on the other hand, it poses the problem of how to rigorously assess the accuracy of the result. Despite the intrinsic difficulty of the problem, the media are full of facial images that have been constructed on the basis of a single given skull. A fascinating survey of such cases can be found in the book of Prag and Neave [2]. The work presented in this paper is part of the ongoing multi-disciplinary project ***.

The traditional facial reconstruction methods are based on manual procedures, producing 2d portraits or 3d sculptures. These methods basically consist of three common steps: (i) equip (a replica of) the raw skull with a sparse set of anatomical landmarks; (ii) apply an average soft tissue thickness to each skull landmark in order to estimate a corresponding landmark on the face; (iii) draw up or sculpt a face fitting the estimated landmarks. Most practitioners add a face muscle model in order to enrich the anatomical accuracy of the reconstruction, leading to the so-called Manchester method described in Wilkinson [1]. The results obtained from forensic art are often quite plausible, as the medical artists may take anatomical, historical, archaeological or other types of expertise into account, giving the observer a feeling of coherence. However, the final result of a manual reconstruction depends on the subjectivity of the artist. Additionally, one single reconstruction requires several days of work of a well-experienced forensic artist, making impracticable the realization of multiple instances and feature variations. In order to alleviate these difficulties, several computer graphic software packages have been developed. These animation software packages use the same methodology as manual methods, allowing the expert to tune some modeling parameters and combine the human expertise with the flexibility of the software, as in Miyasaka *et al.* [3]. However, this approach does not eliminate the subjectivity in the reconstruction. During the last 30 years a large amount of work has been devoted to the conception of objective fully-automated methods. The common pipeline of modern facial reconstruction software is described in Claes *et al.* [4]. First, an expert examines the unknown skull in order to determine anthropological parameters like age, gender and ethnicity. Then a virtual replica of the dry skull is produced and represented according to the modeling parameters. A craniofacial template encoding face, skull and soft tissue information is derived from a head database. Then an admissible geometric transformation drives the adaptation of the craniofacial template onto the unknown skull, according to the 'proximity' between the skulls. As a result, the template face is deformed onto the predicted face associated with the unknown skull, linking together information coming from both the database and the examination of the unknown skull. Finally a skin texture and

hairiness are added to the reconstructed face.

The approach proposed in this article combines classical features - as the anthropological expertise for classifying the unknown skull and the use of a head database - with mathematical and computational skills as 3d geometric modeling. The contribution of this work is threefold. First, a method for generating a closed surface mesh model of the skull template is introduced. The method relies on an original mesh evolution technique. A template shape is iteratively deformed, producing a sequence of shapes that get 'closer and closer' to the source skull. Second, the elastic shape matching method first introduced in *** [5] is used. This technique is used to link skulls (or faces) with each other and learn about their similarities. This procedure is the heart of the reconstruction method and its most original feature. In particular it allows the method to be fully-automated by removing the need of landmarks. Third, the shape matching tool is combined with soft tissue deformation techniques from computational surgery for transporting the skull/face templates onto the unknown skull. The common denominator of the three parts is the use of elasticity equations for driving the shape deformation.

The paper is organized as follows: Section 1 deals with the acquisition and the construction of the database; Section 2 describes the representation of the skull templates; Section 3 presents the method for matching skull and face templates; Section 4 describes the process of reconstruction of the unknown face. In Section 5 some facial reconstructions are presented to prove the efficiency of the approach. Figure 1 summarizes the various steps of the procedure.

1 Data acquisition

Some recent numerical facial reconstruction methods rely on the *a priori* information contained in a database of coupled skull and face templates. The acquisition of both skull and face is accomplished by head CT scans of living subjects, allowing a good visualization of hard tissues. Standard segmentation tools and 3d reconstruction algorithms lead to the definition of dense surfaces of both skull and face from CT data. Unfortunately the invasiveness of this technique causes serious legal and ethical problems, preventing the constitution of a large database of healthy subjects. Due to this difficulty, several studies have proposed to exploit the relationship between soft and hard tissues by means of average soft tissue thickness measurements, for example Tilotta *et al.* [6], Hwang *et al.* [7] and De Greef *et al.* [8].

Soft tissue depth tables are usually used in combination with a large database of face templates as in Claes *et al.* [4]. Facial templates can be acquired by non-invasive techniques such as stereophotogrammetry, Grewe *et al.* [9], making the constitution of a large database painless and easy. However, despite the acquisition of dense surface templates for describing the outer face, the average values of soft tissue thickness are systematically measured on a sparse set (< 53) of (manually positioned) anatomical landmarks. See Vezzetti *et al.* [10] for a review of recent 3D landmark-based facial reconstruction methods. Since the manual measurement is time consuming and requires expertise in correctly identifying the landmarks, it is actually infeasible to extend these measurements to a dense distribution of points. See Kustar *et al.* [11] for a discussion about the use of sparse soft tissue measurements for facial reconstruction purposes. Several authors have claimed the importance of using a dense representation of the soft tissue information, for example by describing the intra-subject correlation in terms of the volume between the two boundary surfaces representing the face and the underlying skull, Nelson and Michael [12], Quatrehomme *et al.* [13]. The results presented in this study are based on a collection of 26 head CT scans of female healthy subjects aged between 20 and 40 years. The CT images used have been provided by the Statistical Facial Reconstruction project of Paris Descartes University presented in Tilotta *et al.* [19]. The 3d reconstruction from tomographic data described in this section, combined with an original wrapping method (see Section 2), allowed us to define closed surface models of both face and skull.

Image segmentation

Data segmentation consists in identifying the bone and soft tissues on stacked 2d gray-level images. This procedure has been carried out

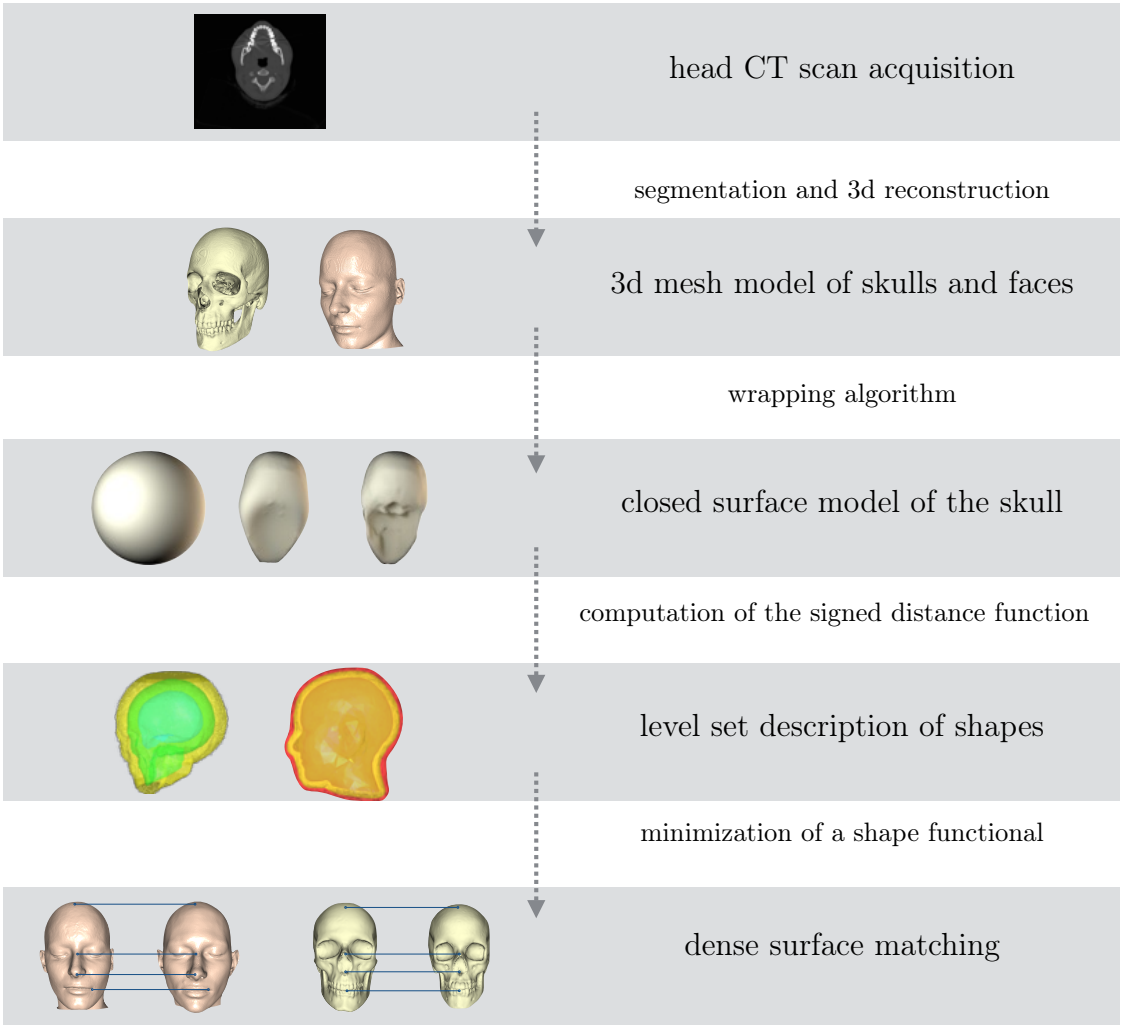

Figure 1 – From CT scans to densely matched surface templates (see Sections 1, 2 and 3).

in a semi-automated way with the help of the software Amira developed by Stalling *et al.* [20]. First, the CT slices are automatically pre-segmented using a multi-threshold technique. This step consists in partitioning the original images into subdomains whose boundaries are identified by given intensity values. The bone and soft tissues threshold values used are described in Tilotta *et al.* [19]. From the pre-segmentation step, two sets of binary images -respectively for bone and soft tissues- are obtained. By stacking these slices one can essentially detect the 3d structures. However the intensity-based segmentation is not enough to ensure a correct separation of the tissues of interest, due to the presence of noise on the data and artefacts occurring during the acquisition process. The binary images are then cleaned by removing the so-called islands (very small structures whose contours are defined by only a few pixels). These structures can be external to the tissues of interest (noise added during the acquisition process) or very thin internal structures (small bones inside the cranium). This action helps denoising the images. Moreover in most of the subjects, large artefacts due to dental filling are observed on the images. These defects need to be manually removed on each affected slice (see Figure 2).

Geometric mesh processing

From the segmented 2d slices, 3d mesh models of the skull and the face are generated by a marching cube algorithm, Stalling *et al.* [20]. These initial meshes contain, in general, a prohibitive number of elements that are redundant and oversampled to correctly describe the geometry of the model. These dense meshes are simplified thanks to the surface remeshing tool *mmgs*, developed by Dapogny *et al.* [21] by a local modification approach. The remeshing procedure aims at providing (i) a correct and accurate geometric approximation of the underlying 3d model (geometric mesh) and (ii) a computational mesh of high quality elements suitable for finite elements simulations (computational mesh). To ensure vicinity between the original and the remeshed triangulations, the remesher controls the discrete Hausdorff distance between the two sets of triangles. The element size of the simplified mesh is locally adapted to the surface curvatures, ensuring a correct approximation of the surface geometry. As illustrated in Figures 3 and 4, this procedure also removes the 'staircase' artefacts due to the spatial discretization and connectivity.

2 Generation of surface model of the skull

The human skull is characterized by a complex structure, showing small details that are difficult to both acquire and handle numerically. Due to these difficulties, several authors opt for describing the skull through underlying anatomical or geometrical substructures. The most popular choice leads to the definition of a sparse set of anatomical landmarks, possibly coupled with a dense representation of the skull, see Claes *et al.* [14], Vandermeulen *et al.* [22] or Knyaz *et al.* [23]. Some authors use automatically detected continuous crest-lines, Quatrehomme *et al.* [13]. The process of matching skull templates is then driven by the outlined feature structures, by requiring their best alignment.

The purpose of this section is to characterize the skull template in terms of a bounded domain, known by a closed mesh of its boundary. This issue is related to the more general problem of surface reconstruction from sample points. Surface reconstruction methods have been extensively investigated in the context of interface evolution via level set methods (see Claisse and Frey [24] and references therein) or via deformable surfaces, as in Duan *et al.* [25] or Miller *et al.* [26]. The specific task, already evoked in Jones [27], Tilotta *et al.* [6], is to define a closed surface of the skull. In order to achieve this goal an original wrapping algorithm based on mesh deformation techniques is proposed. First, a (possibly invalid) source triangulation $\mathcal{T}_S$ of the skull geometry is generated by standard segmentation and 3d reconstruction tools (see Section 1). Then, a closed surface, for example a sphere, is iteratively deformed, producing a sequence of surfaces that are 'closer and closer' to the source triangulation $\mathcal{T}_S$. The final deformed surface partitions the ambient space into two sub-regions defining unambiguously an interior

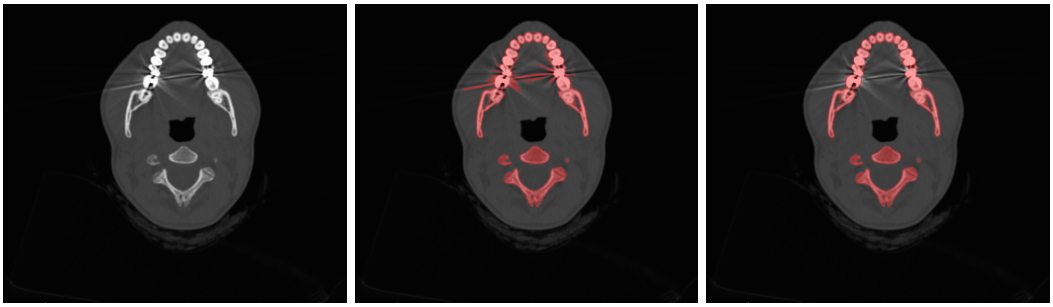

Figure 2 – Left: reference gray-level image. Middle: pre-segmentation of the bone using a threshold technique (red). Right: segmentation of the bone after denoising and artefact removal (red).

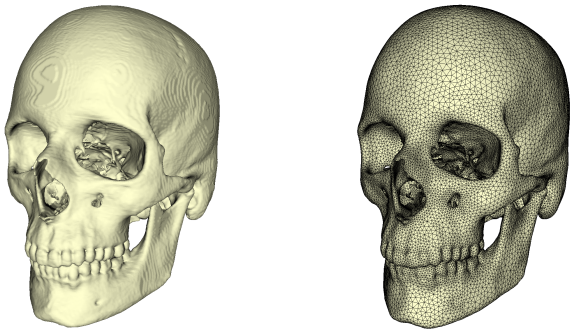

Figure 3 – Left: 3d mesh of the skull after segmentation (2 179 332 triangles). Right: 3d mesh of the skull after geometric remeshing (15 6301 triangles).

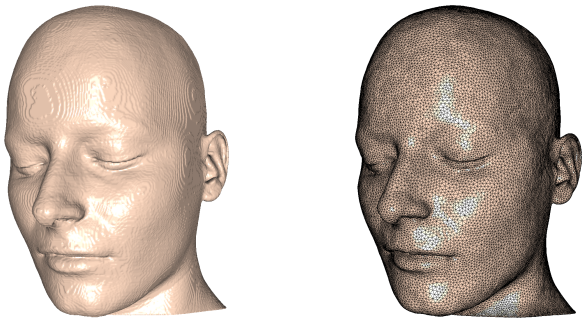

Figure 4 – Left: 3d mesh of the face after segmentation (1 286 542 triangles). Right: 3d mesh of the face after geometric remeshing (90 949 triangles).

(resp. exterior) domain. This preliminary step is of crucial importance for matching shapes among the head database (see Section 3).

Presentation of the method

Let Γ_0 (resp. Γ^0) be the sphere of radius $r > 0$ (resp. $R > r$) and let Ω^0 be the volume between Γ_0 and Γ^0. Suppose that Ω^0 encircles $\mathcal{T}_S$ and is filled with a linear elastic material whose deformation is driven by the Elasticity equations recalled in the box below.

Elasticity equations *The displacement field of a shape Ω clamped at a part Γ^D of its boundary Γ and deflated under the effect of internal pressure $p \in H^{-1/2}(\Gamma^N)$ on $\Gamma^N = \Gamma \setminus \Gamma^D$ is achieved as the unique solution $u \in H^1_{\Gamma^D}(\Omega)^3 := \{w \in H^1(\Omega)^3, w = 0 \text{ on } \Gamma^D\}$ of the following variational problem:*

$$\int_\Omega \sigma(u) : \varepsilon(v)\, dx = \int_{\Gamma_N} pv \cdot n\, ds, \quad (2.1)$$

for all $v \in H^1_{\Gamma_D}(\Omega)^3$, where the stress tensor σ follows the Hooke's law:

$$\sigma(u) = 2\mu\varepsilon(u) + \lambda\ tr(\varepsilon(u))I,$$

with λ, μ the Lamé coefficients and $\varepsilon(u) = \frac{1}{2}(\nabla u + \nabla u^T)$ the linearized strain tensor.

Hence, starting from Ω^0 deflated on its interior boundary Γ_0, a sequence of shapes Ω^k - with interior boundaries Γ_k - is produced. Points of Ω^k are advected according to Equation (2.1) until they intercept the triangulation $\mathcal{T}_S$. Doing so, at each step k the intersection between the vector displacement and the triangulation $\mathcal{T}_S$ is checked. In case of multiple intersection points, the closest point is retained. Whenever a contact between the advecting shape and the source triangulation occurs, the first is clamped and forced not to cross the boundary of the latter.

The advecting sequence of internal boundaries Γ_k gets closer and closer to the source mesh $\mathcal{T}_S$ thanks to the strict inequality:

$$d_H(\Gamma_{k+1}, \mathcal{T}_S) < d_H(\Gamma_k, \mathcal{T}_S),$$

where $d_H(\cdot, \cdot)$ is the Hausdorff distance between the two surfaces. Finally, for k sufficiently large, Γ_k defines a closed boundary that wraps the source triangulation $\mathcal{T}_S$.

Numerical issues

From the numerical point of view, the solution of the Elasticity equations (2.1) is computed by the Finite Elements Method on a volume mesh, that is Ω^0 is filled with tetrahedra. For its part the boundary Γ_0 is discretized as a surface mesh $\mathcal{T}_0$. The iterative algorithm is performed in order to get a sequence $\mathcal{T}_k$ of meshes with decreasing values of $d_H(\mathcal{T}_k, \mathcal{T}_S)$. Given a fixed integer N, the procedure ends if all the points in $\mathcal{T}_k$ have reached $\mathcal{T}_S$ or if N iterations of the process occur without registering a new intersection. The latter condition deals with the potential presence of holes in $\mathcal{T}_S$.

Figures 5 and 6 depict the wrapping of a skull triangulation. The parameters used for Equation (2.1) correspond to a very soft and compressible material. The procedure ends after 35 iterations with $N = 5$, running in a few minutes on a standard laptop computer. About 85% of points on the triangulation $\mathcal{T}_{35}$ are clamped on the surface mesh $\mathcal{T}_S$.

3 Inter-subject shape matching

Shape morphing or matching arises in a wide variety of situations in areas ranging from biomedical engineering to computer graphics. Beyond the specific stakes to each particular application, the general issue is to find one transformation from a given 'template' shape Ω_0 into a 'target' Ω_T (see Figure 7). Such a transformation may be used as a means to appraise how much Ω_0 and Ω_T differ from one another - for instance in shape retrieval, classification or recognition - or to achieve physically the transformation from Ω_0 to Ω_T (in shape registration, reconstruction, or shape simplification). See for instance Veltkamp [28] and references therein for an overview of several related applications. In the facial reconstruction context, shape matching is a key ingredient for studying the shape database, making

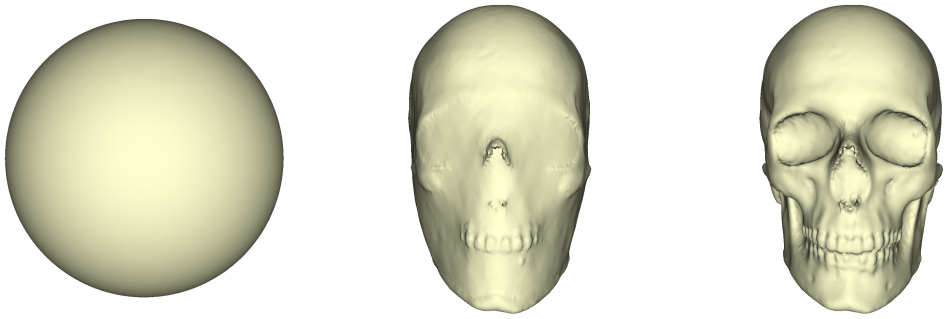

Figure 5 – Left: initial surface Γ_0. Middle: advecting surface Γ_{10}. Right: final surface Γ_{35}.

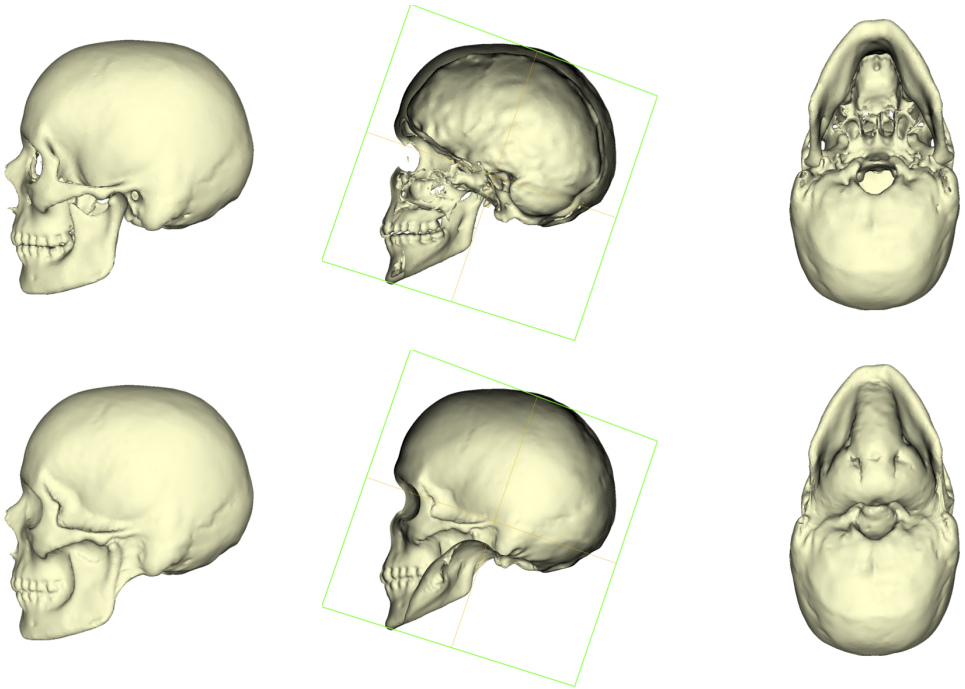

Figure 6 – Top: 3d model of the skull. Bottom: wrapped skull.

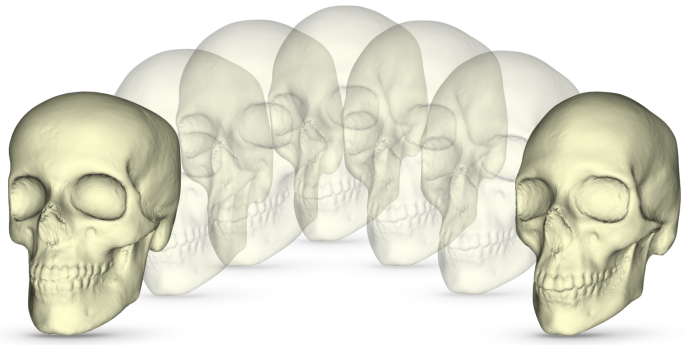

Figure 7 – Elastic shape matching allowing to deform a shape onto another.

possible the generation of average shapes - possibly weighted according to their 'similarity'- as well as for driving the registration of the craniofacial template onto the unknown skull.

The problem is stated as follows: given a 'template' shape Ω_0 and a 'target' shape Ω_T, the aim is to deforme the mesh of Ω_0 onto a computational mesh of Ω_T.

To achieve this purpose, a method that has much in common with that of Bajcsy and Kovacic [29] is proposed, borrowing techniques from shape optimization, and more generally optimal control. Under the assumption that Ω_0 and Ω_T share the same topology, the desired transformation from Ω_0 to Ω_T is obtained through a sequence of elastic displacements, which are obtained by minimizing an energy functional based on the distance between Ω_0 and Ω_T. In this section, the mathematical framework and some numerical issues related to the method are briefly presented. Refer to *** [5] for more details and for 2d and 3d numerical examples.

Presentation of the method

The discrepancy between a reference shape Ω and a target shape Ω_T is measured by the following functional $J(\Omega)$ of the domain:

$$J(\Omega) = \int_{\Omega} d_{\Omega_T}(x)dx, \tag{3.1}$$

which involves the Euclidean *signed distance function* d_{Ω_T} to Ω_T, defined as:

$$d_{\Omega_T}(x) = \begin{cases} -d(x, \partial\Omega_T) & \text{if } x \in \Omega_T, \\ 0 & \text{if } x \in \partial\Omega_T, \\ d(x, \partial\Omega_T) & \text{if } x \in {}^c\overline{\Omega_T}. \end{cases}$$

In the above formula, $d(\cdot, \partial\Omega_T)$ denotes the usual Euclidean distance function to the boundary $\partial\Omega_T$.

In order to decrease the value of $J(\Omega)$, the domain Ω must expand in the regions of the ambient space where d_{Ω_T} is negative (that is, in the regions comprised in Ω_T), and to retract in those where it is positive. Note that the functional $J(\Omega)$ has a unique, global minimizer $\Omega = \Omega_T$, and no extra local minimum point provided Ω_T is connected. It is then expected that an iterative algorithm for minimizing $J(\Omega)$, starting from Ω_0, will lead to an interesting way to transform Ω_0 into Ω_T. This paves the way for an iterative algorithm, producing a sequence $(\Omega_k)_{k=0,\dots}$ of shapes, which are 'closer and closer' to Ω_T: at each step, Ω_k is updated according to

$$\Omega_{k+1} = (I + u)(\Omega_k), \tag{3.2}$$

where u is a suitable descent direction for $J(\Omega)$.

Now, imagine that all the considered shapes Ω are filled with a linear elastic material. One can compute the unique solution u of the elasticity equations (2.1) where the pressure p is taken equal to $-d_{\Omega_T}$. This vector field u is naturally a descent direction for $J(\Omega)$ since, by a classical calculation (see *** [5] for more details), the shape derivative of the function $J(\Omega)$ satisfies

$$J'(\Omega)(u) \leq 0.$$

Numerical issues

For numerical implementation, on the one hand the template shape Ω_0 is filled with tetrahedra and the Elasticity equations are solved on this volume mesh by the Finite Element Method. On the other hand the target shape Ω_T is only supplied through its signed distance function, e.g. as a piecewise affine function on a large computational box.

Starting from the template shape Ω_0, a gradient descent algorithm with adaptive step size is performed in order to get a sequence $(\Omega_k)_{k=0,\dots}$ of domains with decreasing values of $J(\Omega_k)$. The algorithm stops when the step size is smaller than a fixed tolerance. The global mapping from Ω_0 to Ω_T is easily recovered by the composition of the local displacements between each iteration.

In the proposed examples, the calculation of the signed distance function to Ω_T is performed using the algorithm described in Dapogny and Frey [30]. The error is computed as the L^2-norm of the distance d_{Ω_T} calculated on the boundary of the final shape.

Figure 8 depicts the matching of two skull shapes. The convergence of the gradient descent procedure is obtained in 300 iterations and the final error equals 0.1 mm (much smaller than the minimal mesh size), revealing an excellent matching of Ω_{300} with Ω_T.

Next, a face example is considered; see Figure 9. 400 iterations of the gradient descent algorithm have been performed to achieve convergence, running in a few minutes on a standard laptop computer. The error calculated on the boundary of the final shape Ω_{400} is 0.2 mm (again, much smaller than the minimal mesh size).

Remark 3.1. *The ears are not included in the face-matching process, since these structures are not linked with the underlying skull morphology. This procedure is simply done by defining patches on the face template and including only the interesting patches in the minimization of* $J(\Omega)$.

4 Registration of the craniofacial template onto the unknown skull

The parametrization of skull, face and soft tissue information depends strongly on the nature of the database. Using CT scans of living subjects allows a dense representation of the craniofacial information. If closed surface models of both skull and face are available (see Section 2), then the craniofacial template may be described in terms of the 3d domain delimitated by the outer face and the inner skull boundaries, generating a 3d 'mask' that incorporates the soft tissue information. A single craniofacial template may be used for producing templates of all individuals in the database. The procedure relies on the shape matching technique (see Section 3), generating a set of vector fields, one for each individual, each of them allowing to deform the template shape onto a specific shape of the database.

Various methods have been proposed for deforming the craniofacial template onto the unknown skull. On the one hand, template deformation methods use generic mathematical transformations such as radial basis functions (Quatrehomme *et al.* [13]). Care has to be taken because no knowledge of facial anatomy is incorporated in these transformations leading sometimes to awkward looking faces. On the other hand face-specific methods (Claes *et al.* [14], Paysan *et al.* [15], Berar *et al.* [16], Bai *et al.* [17], Duan *et al.* [18]) use Principal Component Analysis on a facial database to generate a statistical shape model. The advantage is that faces are then deformed in a face-specific manner within statistical boundaries. The disadvantage is that the deformations are dependent on the database and can be too restrictive in case of small databases.

Here the method lies on the 'physical' deformation of the craniofacial template onto the unknown skull. This approach allows to overcome the drawbacks which affect existing template deformation methods. The mask is deformed according to a displacement field prescribed on the skull boundary, measuring the deformation of the skull template onto the unknown skull. Under the effect of boundary changes, the mask is allowed to deform as an elastic material, result-

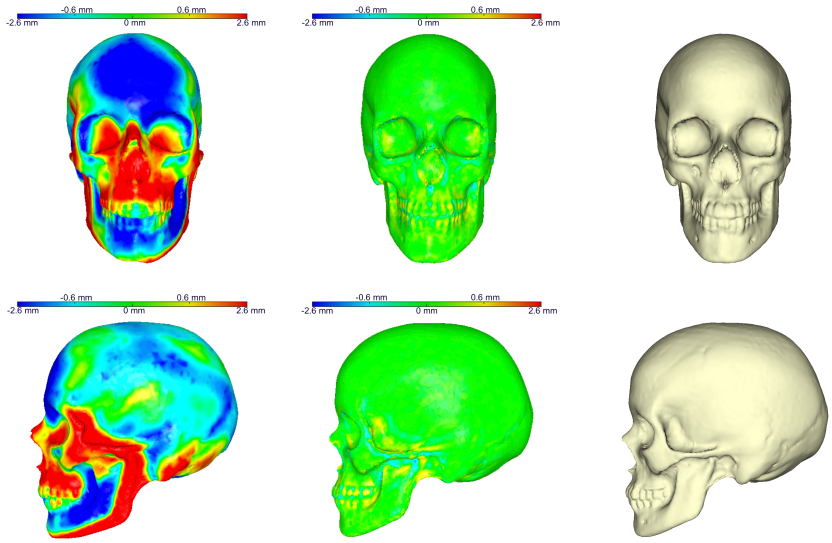

(a) (b) (c)

Figure 8 – (a) Template shape Ω_0 and discrepancy with respect to the target shape. (b) Deformed shape Ω_k for $k = 300$ and discrepancy w.r.t. the target shape. (c) Target shape.

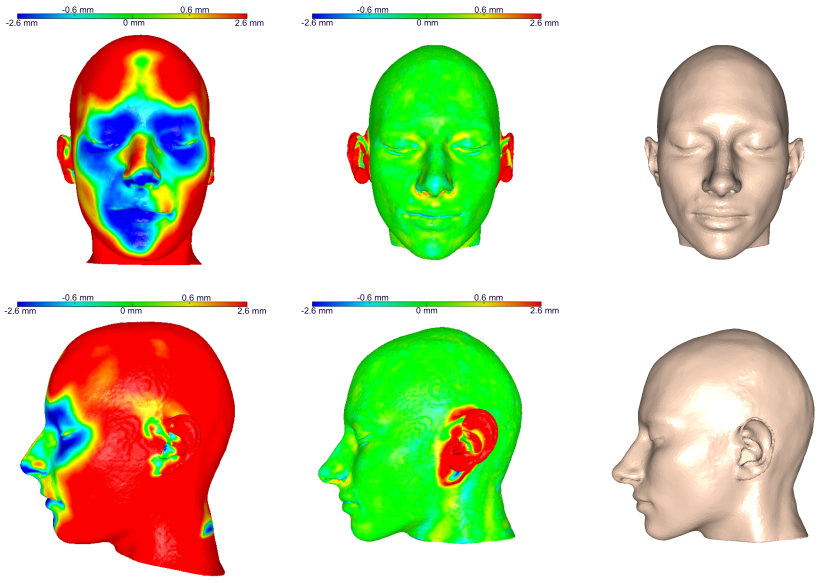

(a) (b) (c)

Figure 9 – (a) Template shape Ω_0 and discrepancy with respect to the target shape. (b) Deformed shape Ω_k for $k = 400$ and discrepancy w.r.t. the target shape. (c) Target shape.

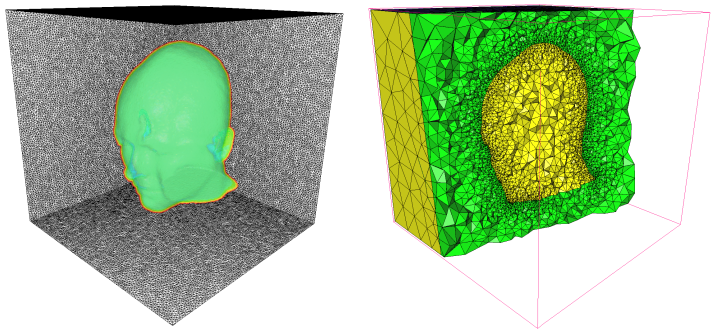

(a) (b)

Figure 10 – (a) Target shape Ω_T as the zero level set of the signed distance function; (b) Adaptive remeshing of the computational box;

ing in a deformed face shape that is now adapted to the unknown skull. The use of elasticity for soft tissue deformation is largely customized in the field of computational maxillofacial surgery, Chabanas *et al.* [31], Zachow *et al.* [32].

Craniofacial template generation

Let $(S_i)_{i=0,\cdots,N}$ and $(F_i)_{i=0,\cdots,N}$ be the collection of skulls and faces of the database. Thanks to the procedure described in Section 2, theses shapes can be at this point considered as closed surfaces. Then, the volume between S_i and F_i can be defined, generating a 3d mask M_i (called craniofacial template).

The craniofacial templates are first roughly aligned by an Iterative Closest Point algorithm. Then, a reference craniofacial template, say M_0, is chosen and filled with an elastic material (see Figure 11). It is matched onto all the $M_1, \cdots, M_N$ (with global displacements $u_1, \cdots, u_N$) thanks to the shape matching process described in Section 3, that is:

$$M_i = (I + u_i)(M_0) \quad \text{for all } i = 1, \cdots, N.$$

See Figure 13.

Note that this process generates meshes for all the craniofacial templates $M_1, \cdots, M_N$ that share the same number of elements (vertices, tetrahedra) and the same connectivity. The computation of average shapes therefore turns into trivial average of the vector fields. Any convex combination w of the form:

$$w = \sum_{i=1}^{N} \alpha_i u_i, \text{ with } \alpha_i \in [0,1] \text{ and } \sum_{i=1}^{N} \alpha_i = 1,$$

defines a new shape W through the mapping:

$$W = (I + w)(M_0).$$

See Figure 12 for an example of generation of new shapes as a convex combination of three templates.

Face-to-skull mapping via skull matching

Now let u_0 be the global displacement mapping the reference skull S_0 onto the target skull S_T. The 3d mask M_i is elastically deformed under the effect of the boundary changes (see Figure 14). The deformation of the template M_i is achieved as the solution U_i of an elastic problem similar to (2.1), in which the displacement condition $U_i = -u_i + u_0$ is imposed on the skull boundary and zero traction conditions on the face boundary. The soft tissue deformation step produces N new faces, each one of them obtained by linking a specific craniofacial template M_i with the unknown skull. These facial items are then combined together to predict the most plausible face associated to the unknown skull.

5 Results and discussion

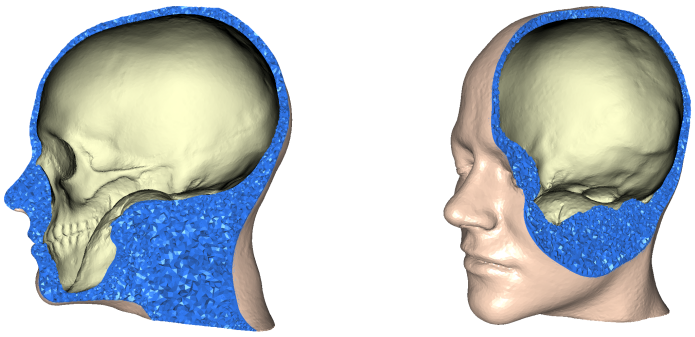

Figure 11 – Generation of a 3d mask encoding soft tissue information.

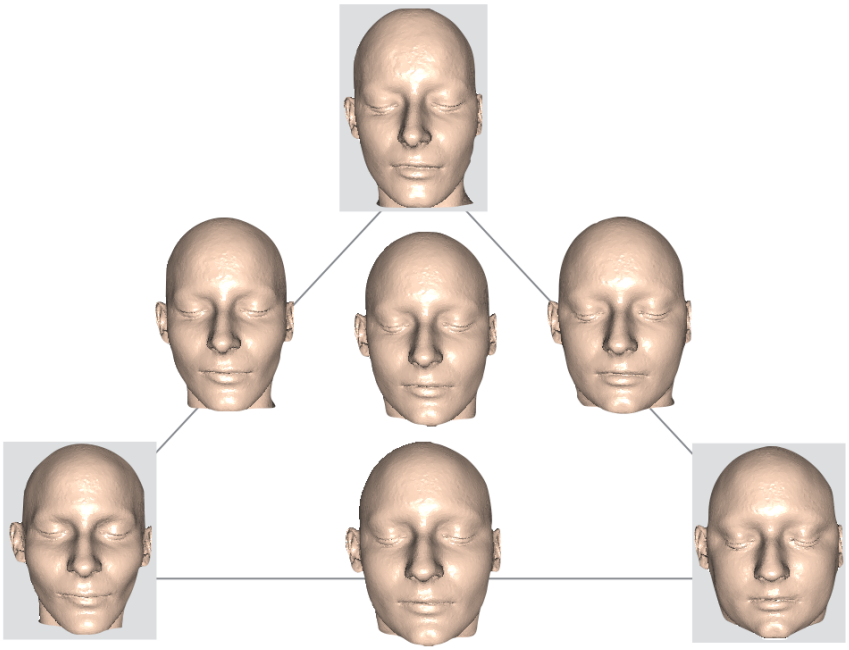

Figure 12 – The corners of the triangle display three faces in the database. The top template is chosen as reference shape and matched onto the bottom right template and the bottom left template. The middle of the triangle and the mid-edges display the 'barycenter' faces computed by averaging the displacement fields.

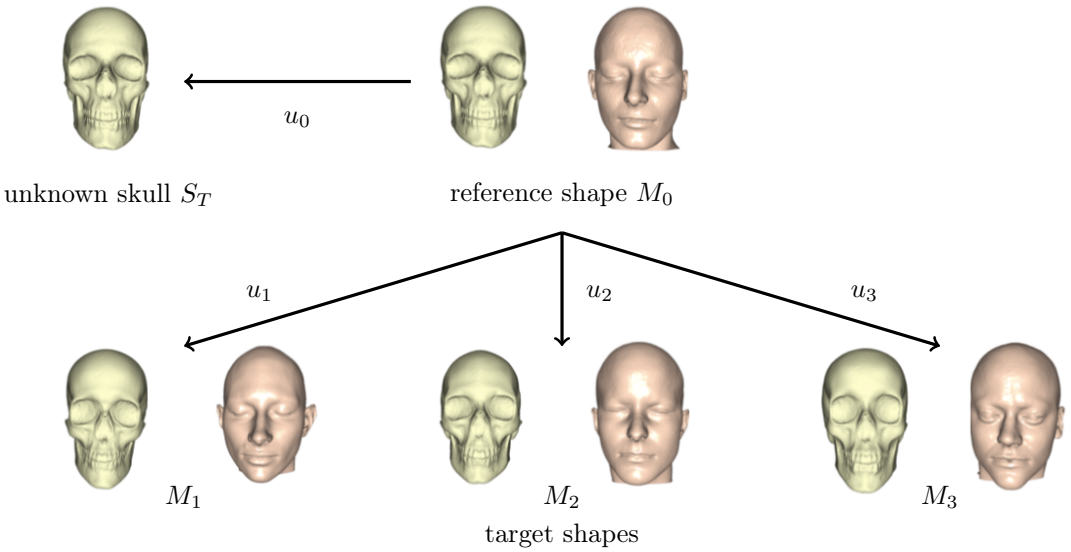

Figure 13 – Matching skull and face templates within the database

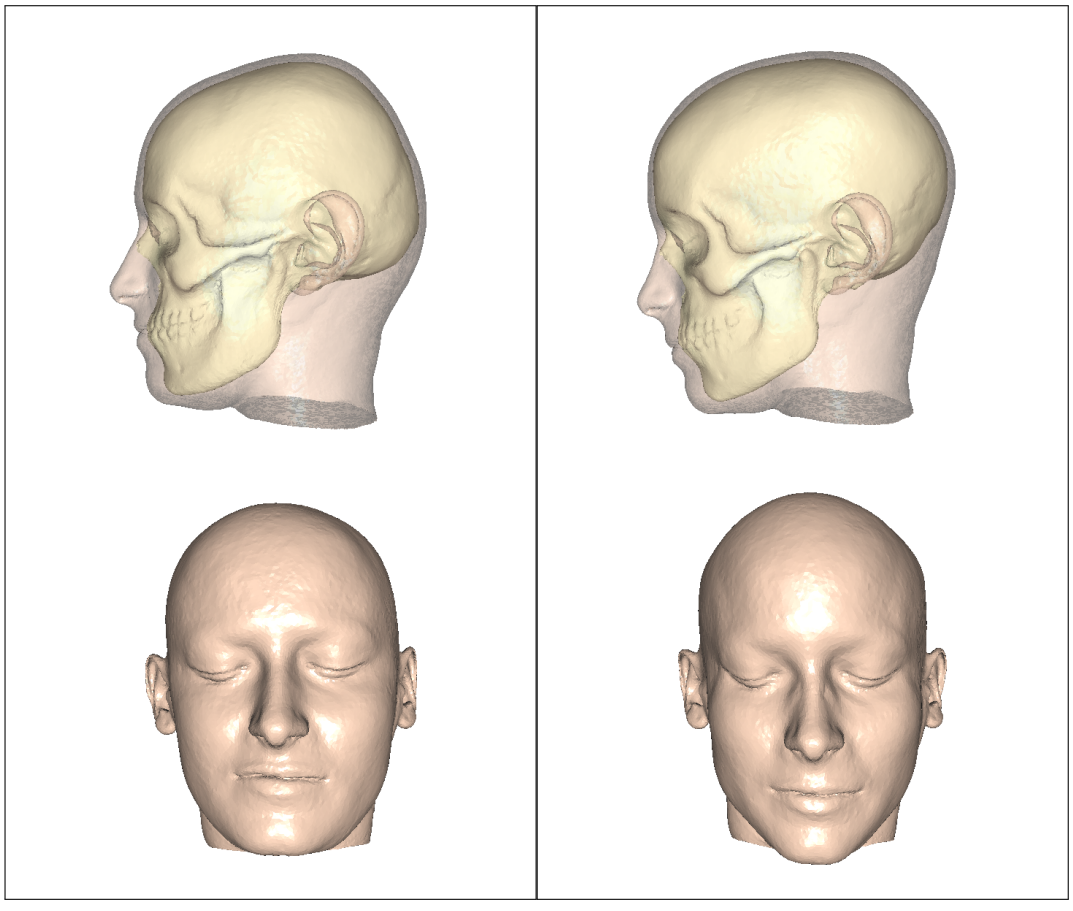

(a) Initial (b) Final

Figure 14 – Elastic deformation of the mask under the effect of skull changes.

Use of facial reconstruction techniques in Forensic Science

An essential deal of the work of a forensic scientist regards the identification of post-mortem bodies. In the special case in which the facial remains are no longer available, the forensic scientist can resort to various techniques to achieve a positive identification of the dead: DNA assessment, dental record analysis, the identification of a tattoo, the serial number of a prosthesis, and other accepted methods of identification. All these techniques are based on a principle of comparison (with respect to a sample or to a database) and can indeed fail in absence of comparative elements. For instance, at the Forensic Medicine Institut in Paris, this situation shows up for 2 up to 5 cases per year. In this context, a facial reconstruction is then the last resort for reaching a positive identification. The key idea is to scan the skeletal remain to generate a virtual replica of the dry skull and to use a facial reconstruction method to produce a virtual estimation of the victim's face. Then, the produced output is compared with a pool of facial photos which contains the actual target and other individuals of similar age and ethnicity. Then, a group of volunteers is asked to choose which face of the pool is the most resemblant to the reconstruction (face pool assessment). In the context of a murder investigation, a call for witnesses can also be demanded. Indeed the reconstructed face should sufficiently resemble to the original victim's face to allow a recognition and enhance a positive identification. For examples of forensic cases which have employed facial reconstruction techniques see the book [2] or the reviews [4, 33]. Actually in France, forensic facial reconstructions are produced using $2d$ reconstruction techniques and are rarely successful. Since a few years our multidisciplinary team works on the conception and development of a open-source software, based on the $3d$ deformation techniques presented in this paper, which will be used during criminal investigations in addition to other endorsed methods. The main concern of this project is to develop a software fully-automatic, usable even by non trained users, and allowing to produce with short time consuming a facial output (or a range of possible outputs) starting from the scan of the unknown skull.

Validation

The validation of a method for facial reconstruction is of tremendous importance to legitimate its use during a criminal investigation. The natural way to address this problem is the "leave-one-out scheme". One individual is removed from the database and the method is employed to reconstruct his/her face given the sole skull. Then the predicted face is compared with the available "unknown face". The discrepancy between the two shapes can be evaluated mathematically by computing distances between them (see below). However, since the final purpose of the method is a positive identification, a *recognition* test can be also employed for revealing the power of prediction of the method, as it is done in Claes *et al.* [4]. A recognition test consists in showing the predicted face together with a sample of faces that contains the unknown face. Then the human volunteer indicates the face (or faces) that is (are) closest to the predicted one. The positive outcome will then correspond to the identification of the unknown face among the sample. Such a study for the method proposed in this article is under process and results will be published in a forthcoming paper.

Hereafter three examples of reconstruction are presented. According to the leave-one-out scheme, one individual is removed from the database and a prediction of his face is generated. Figures 15, 16 and 17 show the results obtained by computing the mean of all the faces transported onto the unknown skull. Figure 18 shows the distribution of the error (signed distance function) over the surface for the three reconstructions. Remark that in the regions of interest, excluding ears, neck and eyes in particular, the error is less than 1 millimeter for most points. Also notice that in these regions, the thickness of the tissue is underestimated or overestimated. Using the information coming from the BMI of the individuals in the database could be a way to propose different reconstructed faces corresponding to different BMI of the unknown individual.

The discrepancy $\mathcal{D}$ between a surface Γ and a reference surface Γ_0 can also be evaluated by the

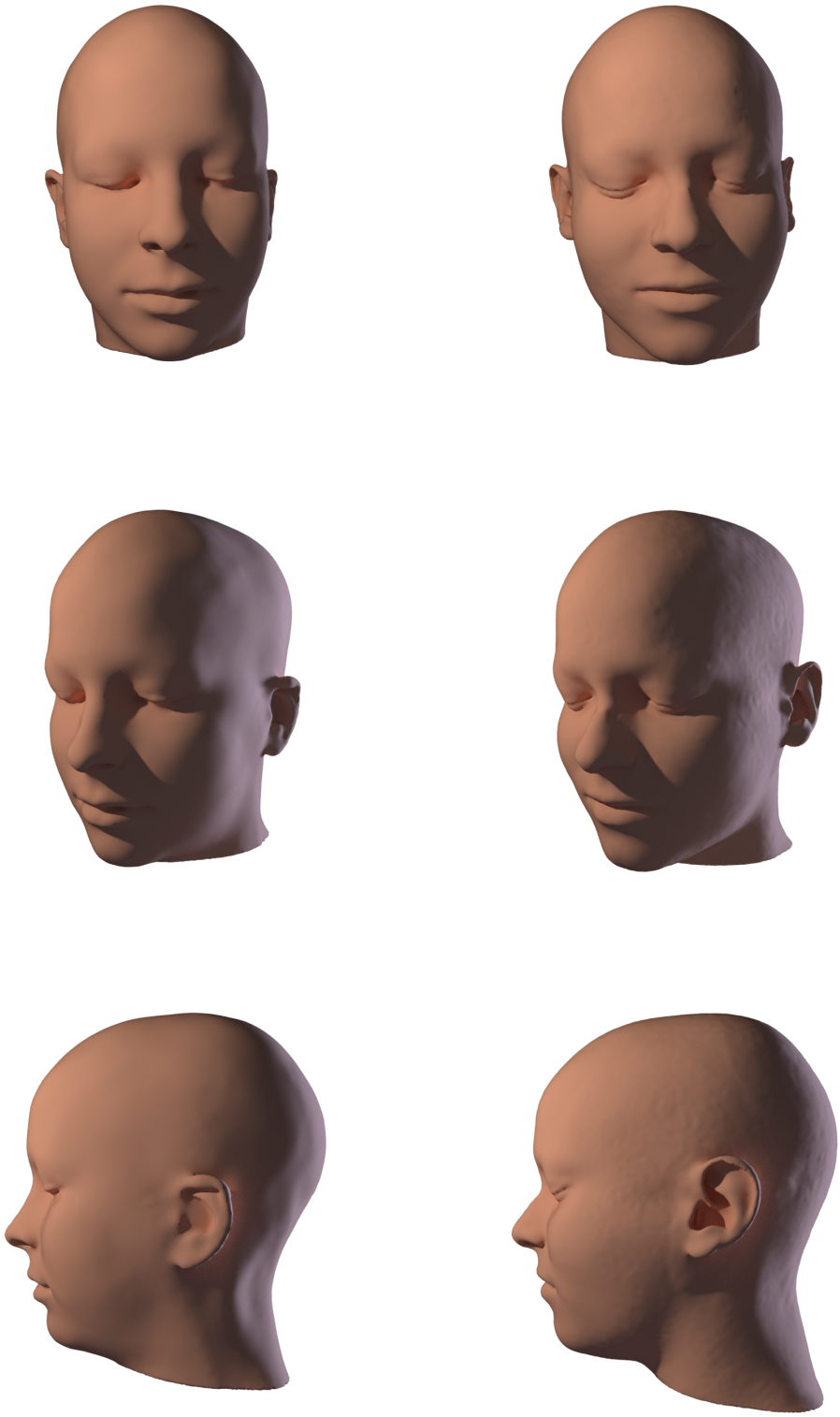

(a) (b)

Figure 15 – Test case 1: (a) Original face. (b) Reconstructed face.

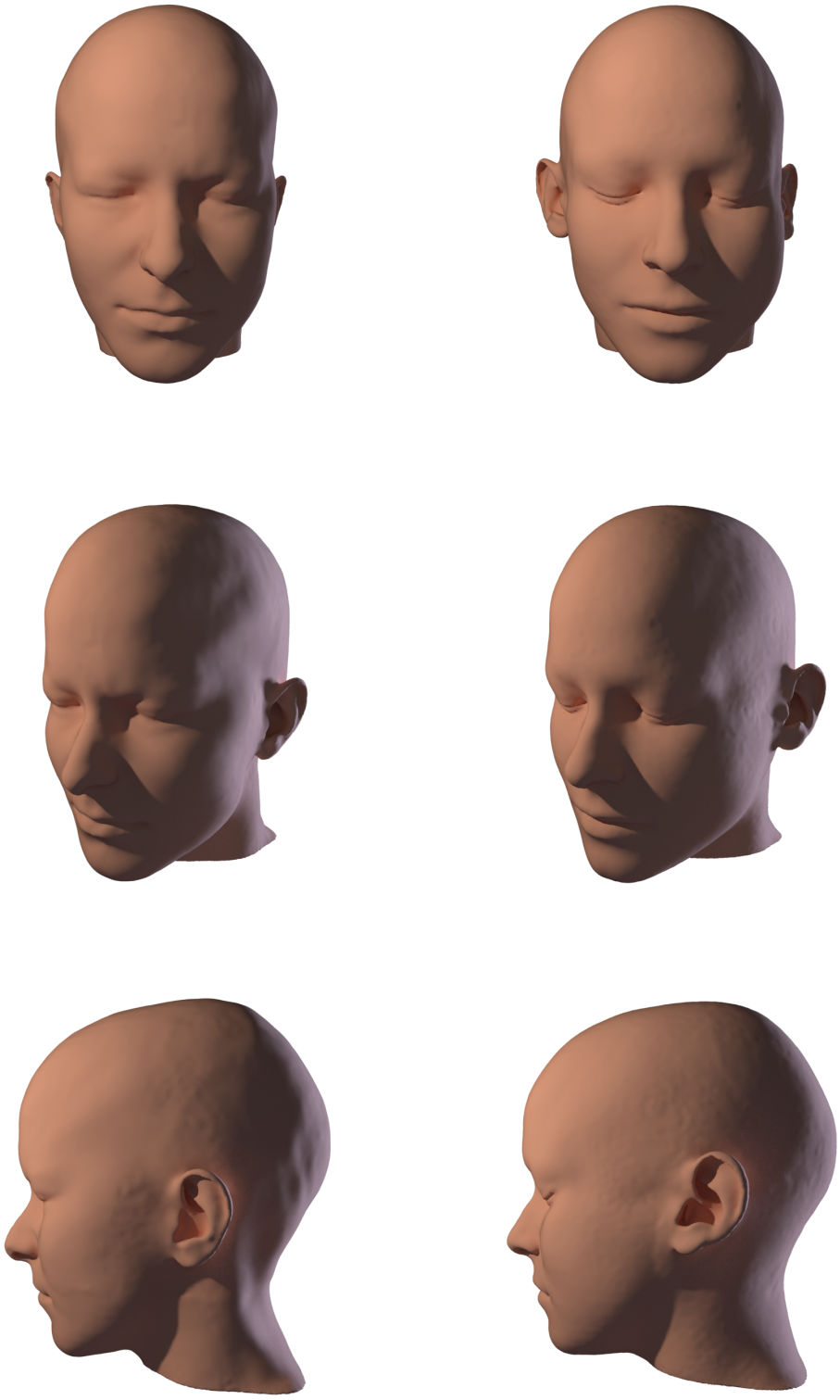

(a) (b)

Figure 16 – Test case 2: (a) Original face. (b) Reconstructed face.

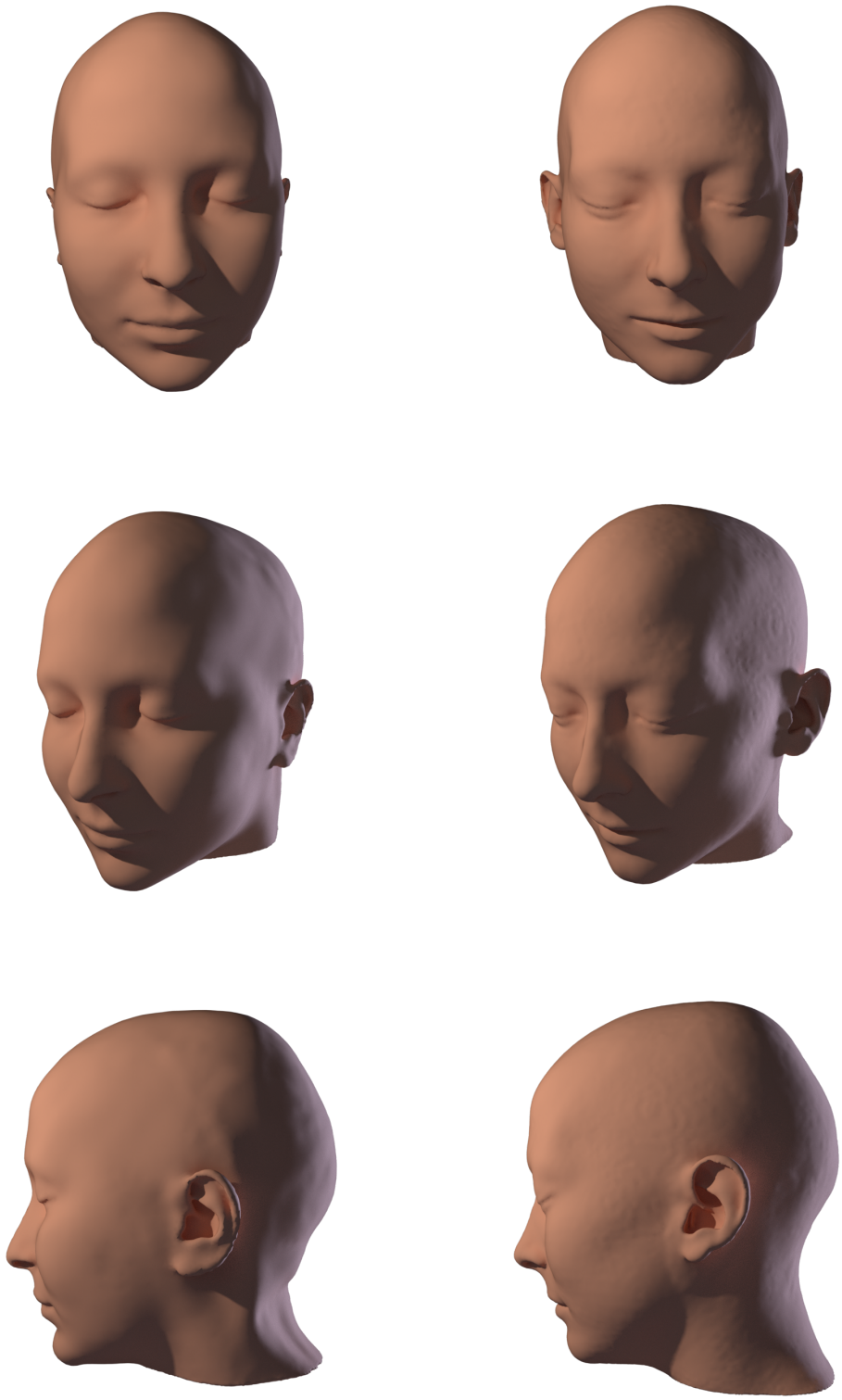

(a) (b)

Figure 17 – Test case 3: (a) Original face. (b) Reconstructed face.

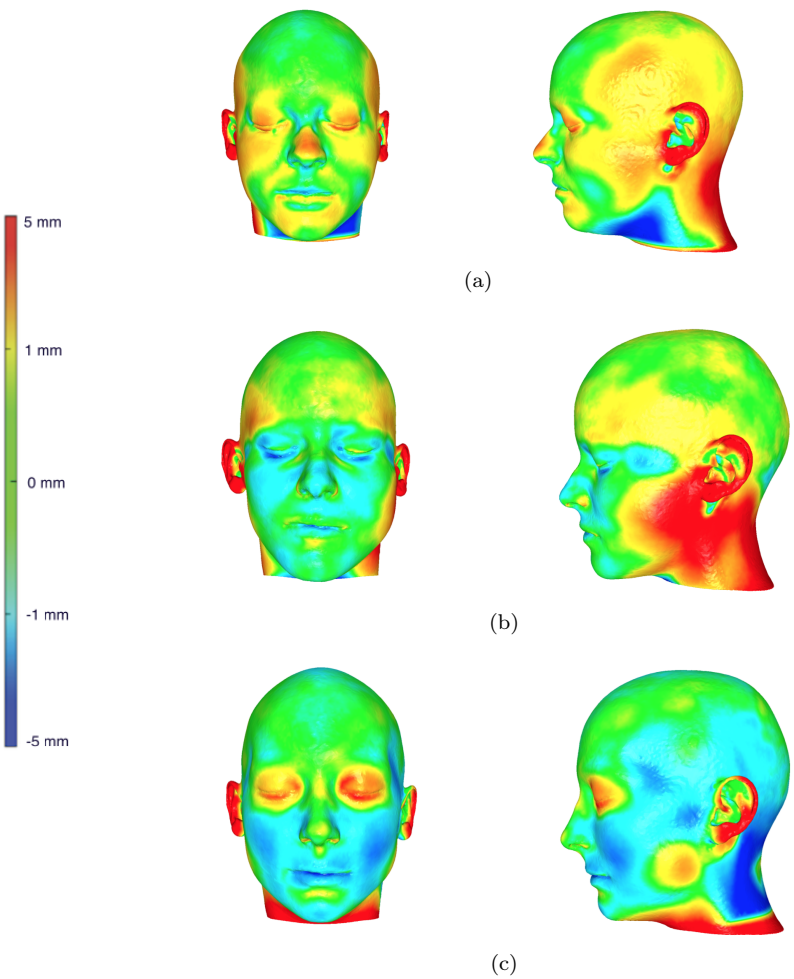

Figure 18 – Discrepancy between the reconstructed and the original faces (a) for the test case 1 of Figure 15; (b) for the test case 2 of Figure 16; (c) for the test case 3 of Figure 17.

following mean error:

$$\mathcal{D} = \left(\frac{1}{|\Gamma|} \int_{\Gamma} d^2(x, \Gamma_0) dx \right)^{\frac{1}{2}},$$

where $|\Gamma|$ is the measure of Γ and $d(\cdot, \Gamma_0)$ is the Euclidean distance to Γ_0. This error estimator is used for evaluating the vicinity between:

1. the skull templates of the database and the unknown skull;
2. the face templates of the database and the unknown face associated with the unknown skull;
3. the face templates after deformation onto the unknown skull and the unknown face associated with the unknown skull;
4. the face templates of the database and the reconstructed average face.

The minimal, maximal and mean values of $\mathcal{D}$ for the 25 templates of the database are reported in Table 1 in each of the third cases. In particular, the discrepancy between a face template and the unknown face is smaller after deformation for all the individuals. Thus, the elastic transformation used in the method seems to be a good tool to transport the faces close to the unknown face. Moreover, the discrepancy between the unknown face and the predicted face is smaller than the discrepancy with any individual in the database, so this measure $\mathcal{D}$ can be used for an automatic numerical identification.

Comparison with previous works

A comparison with previous facial reconstruction methods is a quite hard task. The reliability of two methods should be compared starting from the same database and the same test cases, to avoid the dependencies of the methods on the data. Such a comparison is out of the scope of this paper. Here we limit ourselves to compare the results of the test cases with the outcomes of some statistical facial reconstruction methods referenced in the literature [14, 6, 22]. In Claes *et al.* [14] a statistical method is developed for the purpose of estimating a facial outcome using landmarks. The experiment is carried out from a database of 118 individuals. The mean reconstruction error registered equals 1.4 millimeters, with a standard deviation of 1.04 millimeters. In Vandermeulen *et al.*[22] a statistical method based on implicit surfaces was employed for the facial reconstruction test using a database of 20 individuals. The mean error registered equals 1.9 mm with a standard deviation of 1.7 mm. In Tilotta *et al.* [6] a local technique based on surface patches is used for statistically predicting some facial regions. The experiment is carried out using a database of 47 individuals. For both chin region and nasal region, the mean reconstruction equals 0.99 mm, ranging from 0.58 millimeters to 1.83 millimeters for the nose, and from 0.21 millimeters to 2.41 millimeters for the chin. The mean error registered with the method proposed in this paper is reported in Table 1. Note that most of the error is concentrated on the ears, the neck, the eyes and lips regions. The distribution map of Figure 18 shows that for the three studied test cases the mean error over the remaining regions is smaller than 1 millimeter. The result is similar to the one reported in Tilotta *et al.* [6] (which only deals with the reconstruction of two facial regions) and improves the outcomes of Claes *et al.* [14] and Vandermeulen *et al.*[22], at least when considering the regions of interest. Also, note that all the experiments were conducted on a smaller database and with no need of landmarks, resulting in a significant improvement in the fastness and feasibleness of the overall process, and avoiding manual intervention.

Conclusion

The proposed reconstruction method lies on the 'physical' deformation of templates of coupled faces and skulls onto the unknown target skull. In practice, the acquisition of full head scans of healthy subjects is still a difficult process. Most of the time one can have access to clinical data, meaning that the patients present morphological anomalies or that the scans are only partial (in the case of maxillo-facial examination for surgery purposes). The access to an adequate database of full heads of healthy subjects would enormously improve the final product of the method. Even if the experiments were carried out on a

Test case 1: Discrepancy between ···	min	mean	max
(1) skulls of the database and the unknown skull	5.44 mm	7.86 mm	13.46 mm
(2) faces of the database and the unknown face	5.02 mm	8.94 mm	15.69 mm
(3) faces after deformation and the unknown face	2.93 mm	5.8 mm	10.35 mm
(4) faces of the database and the predicted face	4.54 mm	7.03 mm	11.28 mm

Test case 2: Discrepancy between ···	min	mean	max
(1) skulls of the database and the unknown skull	4.01 mm	7.01 mm	11.1 mm
(2) faces of the database and the unknown face	4.41 mm	7.16 mm	11.4 mm
(3) faces after deformation and the unknown face	2.6 mm	5.3 mm	8.69 mm
(4) faces of the database and the predicted face	3.5 mm	7.65 mm	13.39 mm

Test case 3: Discrepancy between ···	min	mean	max
(1) skulls of the database and the unknown skull	4.46 mm	9.57 mm	17.3 mm
(2) faces of the database and the unknown face	4.92 mm	7.82 mm	13.5 mm
(3) faces after deformation and the unknown face	3.04 mm	5.01 mm	10.6 mm
(4) faces of the database and the predicted face	3.63 mm	8.2 mm	15.15 mm

Table 1 – Discrepancy between shapes for the test cases 1, 2 and 3 of Figures 15, 16 and 17.

small collection of 26 individuals, the preliminary results produced are very promising. The proposed method for shape matching allows an accurate registration. The method is simple to implement and does not require any a priori landmark correspondence, allowing for an automatic processing of the database.

Acknowledgements

***

References

[1] Wilkinson C. Computerized forensic facial reconstruction: A review of current systems. Forensic Science, Medicine and Pathology. 2005;1(3):173–177.

[2] Prag J, Neave R. Making Faces: Using Forensic and Archaeological Evidence. The Trustees of the British Museum. 1997.

[3] Miyasaka S, Yoshinoa M, Imaizumia K, Seta S. The computer-aided facial reconstruction system. Forensic Science International. 1995;74:155–165.

[4] Claes P, Vandermeulen D, De Greef S, Willems G, Clement JG, Suetens P. Computerized craniofacial reconstruction: Conceptual framework and review. Forensic Science International. 2010;201(1-3):138–45.

[5] ***. 2016.

[6] Tilotta FM, Glaunès JA, Richard FJP, Rozenholc Y. A local technique based on vectorized surfaces for craniofacial reconstruction. Forensic Science International. 2010;200(1-3):50–59.

[7] Hwang HS, Park MK, Lee WJ, Cho JH, Kim BK, Wilkinson C. Facial Soft Tissue Thickness Database for Craniofacial Reconstruction in Korean Adults. Journal of Forensic Science. 2012;57(6):1442–1447.

[8] De Greef S, Claes P, Vandermeulen D, Mollemans W, Suetens P, Willems G. Large-scale in-vivo Caucasian facial soft tissue thickness database for craniofacial reconstruction. Forensic Science International. 2006;159(1):126–146.

[9] Grewe CM, Schreiber L, Zachow S. Fast and Accurate Digital Morphometry of Facial Expressions. Facial Plastic Surgery. 2015; 31(5):431–438.

[10] Vezzetti E, et al. Facial Landmarks for Forensic Skull-Based 3D Face Reconstruction: A Literature Review. International Conference on Augmented Reality, Virtual Reality and Computer Graphics. 2016.

[11] Kustár A, Forró L, Kalina I, Fazekas F, Honti S, Makra S, Friess M. FACE R A 3D Database of 400 Living Individuals Full Head CT and Face Scans and Preliminary GMM Analysis for Craniofacial Reconstruction. Journal of Forensic Science. 2013; 58(6):1420–1428.

[12] Nelson LA, Michael SD. The application of volume deformation to three dimensional facial reconstruction: A comparison with previous techniques. Forensic Science International. 1998;94(3):167–181.

[13] Quatrehomme G, Cotin S, Subsol G, Delingette H, Garidel Y, Grévin G, Fidrich M, Bailet P, Ollier A. A Fully Three-Dimensional Method for Facial Reconstruction Based on Deformable Models. Journal of Forensic Science. 1997;42(4):649–652.

[14] Claes P, Vandermeulen D, De Greef S, Willems G, Clement JG, Suetens P. Craniofacial reconstruction using a combined statistical model of face shape and soft tissue depths: Methodology and validation. Forensic Science International. 2006;159:147–158.

[15] Paysan P, L'uthi M, Albrecht T, Lerch A, Amberg B, Santini F, Vetter T. Face reconstruction from skull shapes and physical attributes. Lecture Notes in Computer Science, Pattern Recognition. 2009:232-241.

[16] Berar M, Desvignes M, Bailly G, Payan Y. 3d semi-landmark-based statistical face reconstruction. CIT. 2006;14(1):31?43.

[17] Bai F, Cheng Z, Qiao X, Deng Q, Duan F, Tian Y. Face Reconstruction from Skull Based on Least Squares Canonical Dependency Analysis. IEEE International Conference on Systems, Man and Cybernetics. 2016.

[18] Duan F, Huang D, Tian Y, Lu K, Wu Z, Zhou M. 3D face reconstruction from skull by regression modeling in shape parameter spaces. Neurocomputing. 2015;151(2):674–682.

[19] Tilotta FM, Richard FJP, Glaunès JA, Berar M, Gey S, Verdille S, Rozenholc Y, Gaudy JF. Construction and analysis of a head CT-scan database for craniofacial reconstruction. Forensic Science International. 2009;191(1-3):1–112.

[20] Stalling D, Westerhoff M, Hege HC. Amira: a Highly Interactive System for Visual Data Analysis. The Visualization Handbook. 2005;749–767.

[21] Dapogny C, Dobrzynski C, Frey P. Three-dimensional adaptive domain remeshing, implicit domain meshing and applications to free and moving boundary problems. J. Comput. Phys. 2014;262:358–378.

[22] Vandermeulen D, Claes P, Loeckx D, De Greef S, Willems G, Suetens P. Computerized craniofacial reconstruction using CT-derived implicit surface representations. Forensic Science International. 2006;159(1):164–174.

[23] Knyaz VA, Zheltov SY, Stepanyants DG, Saltykova EB. Virtual face reconstruction based on 3D skull model. Proc. SPIE Three-Dimensional Image Capture and Applications V. 2002;4661:182–190.

[24] Claisse A, Frey P. A nonlinear PDE model for reconstructing a regular surface from sampled data using a level set formulation on triangular meshes. Journal of Computational Physics. 2011;230(12):4636–4656

[25] Duan Y, Yang L, Qin H, Samaras D. Shape Reconstruction from 3D and 2D Data Using PDE-Based Deformable Surfaces. European Conference on Computer Vision. 2004;238–251.

[26] Miller J, Breen D, Lorensen W, O'Bara R, Wozny M. Geometrically Deformed Models: A Method for Extracting Closed Geometric Models Form Volume Data. Proceedings of the 18th annual conference on Computer graphics and interactive techniques. 1991;217–226.

[27] Jones MW. Facial Reconstruction Using Volumetric Data. International Vision Modeling and Visualisation Conference. 2003.

[28] Veltkamp RC. Shape matching: Similarity measures and algorithms. IEEE Shape Modeling and Applications. 2001;188–197.

[29] Bajcsy R, Kovacic S. Multiresolution elastic matching. Computer Vision, Graphics and Image Processing. 1989;46:1–21.

[30] Dapogny C, Frey P. Computation of the signed distance function to a discrete contour on adapted triangulation. Calcolo. 2012;49(3):193–219.

[31] Chabanas M, Luboz V, Payan Y. Patient specific finite element model of the face soft tissues for computer-assisted maxillofacial surgery. Med Image Anal. 2003;7(2):131–51.

[32] Zachow S, Gladiline E, Hege HC, Deuflhard P. Finite-Element Simulation for Soft Tissue Prediction. Computer Assisted Radiology and Surgery. 2000;23–28.

[33] Wilkinson C, Facial reconstruction: anatomical art or artistic anatomy ? J. Anat. 2010;216:235–250.